

## Short-Range Tests of Gravitational Physics

Holly Leopardi and David Smith  
Department of Physics and Astronomy  
Humboldt State University  
One Harpst Street  
Arcata, CA 95521-8299 USA

Faculty Advisor: Dr. C.D. Hoyle, Jr.

### Abstract

Due to the incompatibility of the Standard Model and General Relativity, tests of gravity remain at the forefront of experimental physics research. At Humboldt State University, undergraduates and faculty are developing an experiment that will test gravitational interactions below the 50-micron distance scale. The experiment will measure the twist of a torsion pendulum as an attractor mass is oscillated nearby in a parallel-plate configuration, providing a time varying torque on the pendulum. The size and distance dependence of the torque variation will provide means to determine deviations from accepted models of gravity on untested distance scales. To observe the twist of the pendulum inside the vacuum chamber, an optical system with nano-radian precision is required. Improvements made to the optical autocollimator system that now achieves the required sensitivity, as well as recent data taken with this updated system are discussed. In addition, an overview of an adapted Michelson interferometer is being developed as an entirely new optical system. This system will potentially offer a dramatic increase in the ability to measure small changes in the angle of the torsion pendulum.

**Keywords:** Gravity, Relativity, Optics, Interferometer

### 1. Motivation and Background

Gravity is currently at the forefront of physics research as there has been a push to find a unified theory which would unite the Standard Model and General Relativity. General Relativity (GR) successfully describes gravity and has passed all current experimental tests; however, it is inconsistent with the Standard Model of quantum physics which successfully describes the interactions of the three other fundamental forces. The Weak Equivalence Principle (WEP) is a key component of GR, and violations of it at any length scale would call for a new model of gravity. Some models of String Theory<sup>1,2</sup> predict additional dimensions that would unify the Standard Model and General Relativity. These additional dimensions may alter the gravitational Inverse-Square Law (ISL) a measurable amount on sub-millimeter distance scales. Short range gravity may also provide an explanation for Dark Energy as some theories predict that gravity turns off on scales 0.1 mm and below<sup>3</sup>.

Deviations from the ISL can be modeled using the Yukawa addition<sup>4</sup> to the Newtonian potential energy experienced between two point masses,  $m_1$  and  $m_2$ , separated by a distance  $r$ :

$$V(r) = -\frac{Gm_1m_2}{r} \left(1 + \alpha e^{-r/\lambda}\right), \quad (1)$$

where  $G$  is the universal gravitation constant,  $\alpha$  is a dimensionless constant corresponding to the strength of any deviation from the Newtonian potential, and  $\lambda$  is the length scale at which deviations from the ISL might occur.

Previous experiments<sup>3,5,6</sup> have tested and eliminated the shaded portions of Figure 1, which is a plot of the Yukawa potential in  $\alpha$ - $\lambda$  parameter space. The unshaded portion of Figure 1 shows separations that have yet to be tested and the predicted length scales where deviations may occur. The experiment at Humboldt State University (HSU) is expected to be sensitive to smaller deviations at shorter separations. The predicted HSU experimental sensitivity is represented by the dashed lines which are discussed in Section 2.

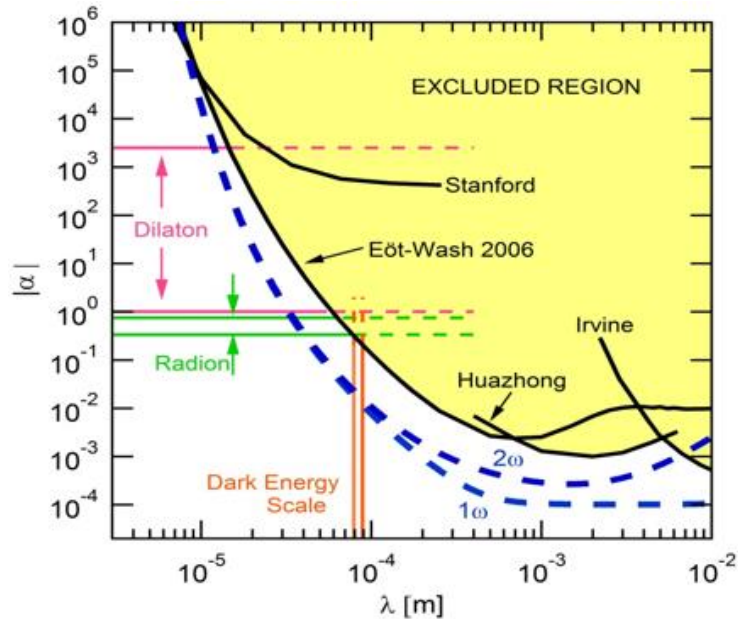


Figure 1. Current and predicted constraints on the ISL in Yukawa potential parameter space

Figure 1 shows current constraints on deviations from the ISL in  $\alpha$ - $\lambda$  Yukawa parameter space. The shaded corner has been excluded at a 95% confidence level by previous experiments<sup>3,5,6,7</sup>. The dashed line is the predicted sensitivity of the HSU experiment, which for some values of  $\lambda$  is an improvement from previous experiments by a factor of 50. Also shown are curves for various theoretical predictions<sup>4</sup>.

## 2. HSU Gravitational Research Laboratory

An experiment to test short-range gravitational interactions between objects separated by 50 microns and below is being developed at the Humboldt State University Gravitational Research Laboratory. This experiment uses a torsion pendulum which separates the experiment from terrestrial gravity. Due to the weakness of gravity, any experimental set-up must be isolated to reduce any environmental noise that could overwhelm gravitational effects. The experimental apparatus is housed inside a vacuum chamber which is pumped down to  $10^{-6}$  Torr and placed in an isolated, thermally-controlled room to reduce thermal and vibrational noise. An overview diagram of the experimental setup is shown in Figure 2.

An ideal experiment would be a null experiment where effects from ordinary Newtonian physics are suppressed and any effects due to short-range gravitational interactions are enhanced. If a test mass were interacting with an infinite plane of matter, the Newtonian gravitational force between the test mass and the plane would not depend on the distance between them due to Gauss' Law. By using a parallel-plate planar torsion pendulum and a much larger attractor plate, this effect can be mimicked. A simplified geometry of the pendulum and attractor mass is shown in Figure 3. The pendulum is suspended from a 20  $\mu$ m-diameter tungsten fiber mounted on a magnetic damper to reduce any oscillations caused by external disturbances. The pendulum's twist is measured optically by a laser reflected off of its polished surface. The beam then returns to an optics block where the deflection of the beam is measured using a position sensitive detector. The signal is digitized and processed to determine the harmonic

amplitude of the twist of the pendulum. The twist amplitude will be compared to the expected Newtonian and Yukawa twist amplitudes and limits in  $\alpha$ - $\lambda$  parameter space will be obtained. Any deviation from the expected ISL or WEP values could be an indication of unobserved properties of gravity or new forces.

The separation between the pendulum and attractor mass,  $s$ , is varied by moving the attractor at the angular drive frequency  $\omega$ . In the approximation of an infinitely large attractor mass, the position of the attractor mass does not affect the twist of the pendulum, whereas any short range interactions will cause more torque on the high density step of the pendulum causing a variation in the pendulum's twist at the attractor modulation frequency. The attractor drive frequency is chosen at a frequency different from the pendulum's resonant angular frequency so that the measured angular twist will be due to the modulation of the attractor mass and not excessively contaminated by external disturbances which could also excite resonant motion in the pendulum. Thus this experiment will not be sensitive to the pendulum's natural mode of oscillation. However, the signal for short range effects is at the same frequency as the attractor drive frequency which could cause systematic error. By making the steps of the parallel plate pendulum out of two materials with different densities but with steps of equal mass, the WEP can be tested. If the attractor mass causes more torque on one of the steps, the WEP will be violated as it states all objects fall at the same rate in a gravitational field regardless of composition. Since both the WEP and the ISL deviations would cause short range torque on the pendulum extra tests would need to be performed with pendulums of differing composition to see if the deviation was due to the ISL or WEP. For an ISL violation the same angular twist of the pendulum would be measured regardless of the material, where for a WEP violation the pendulum's twist would vary with composition.

The  $1\omega$  and  $2\omega$  dashed lines in Figure 1 correspond to the signal produced by the pendulum at the harmonics of the attractor modulation frequency. Figure 4 compares the expected Newtonian torque on the pendulum and the theoretical Yukawa torque as a function of the pendulum-attractor separation distance,  $s$ . From the table in Figure 4, which shows the torque amplitudes at the harmonics for a Newtonian and Yukawa signal, the Newtonian signal is approximately simple harmonic and occurs mainly at  $1\omega$  as do any systematic effects. At higher harmonics the Newtonian signal and any signal from systematic effects is greatly reduced while the Yukawa torque is still measurable. By analyzing the pendulum's torque at higher harmonics of the attractor modulation frequency, any short-range interactions can be distinguished from Newtonian or systematic false effects.

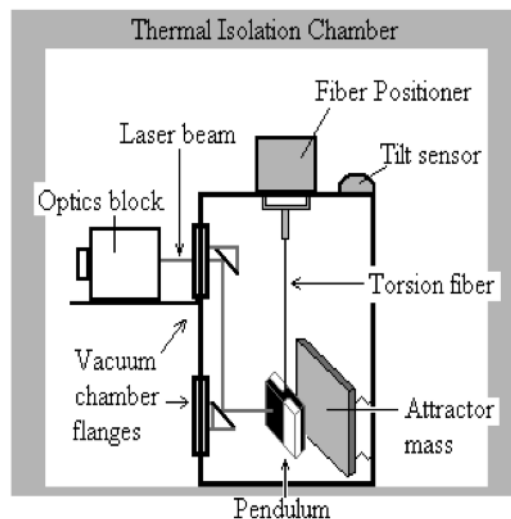


Figure 2. Experimental setup overview

The diagram in Figure 2 shows the experimental setup. A laser enters the vacuum chamber through a window and is directed down to the pendulum via periscopic mirrors. The separation between the pendulum and attractor mass is varied by moving the attractor at the angular drive frequency  $\omega$ . The angular twist of the pendulum at the attractor modulation frequency is measured via the deflection of the laser beam.

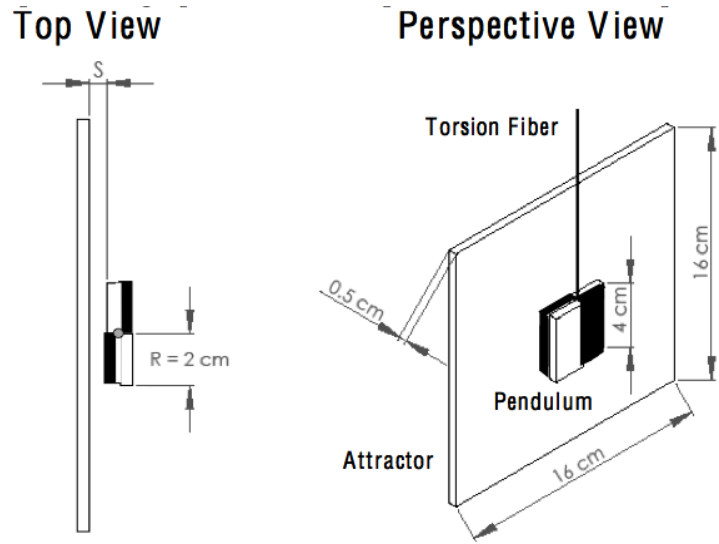


Figure 3. Parallel plate torsion pendulum and attractor mass setup

The parallel plate torsion pendulum and the positioning of the attractor mass is shown in Figure 3. The white indicates the section of the pendulum constructed of aluminum and the black indicates a titanium step. By varying the distance,  $s$ , between the pendulum and the attractor mass at the attractor modulation frequency, the angular twist of the pendulum can be measured to search for deviations from Newtonian gravity. For a null result of the ISL and WEP, there would be no pendulum twist at the attractor modulation frequency.

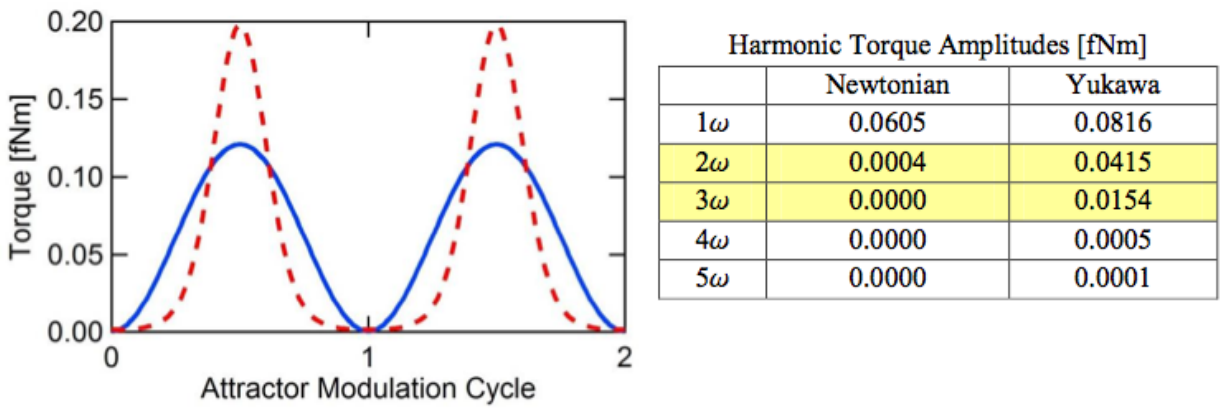


Figure 4. Calculated Newtonian and theoretical Yukawa torques as a function of time and harmonic torque amplitudes

The left side of Figure 4 shows the calculated Newtonian and theoretical Yukawa torques produced on the pendulum as a function of time for two attractor modulation cycles with a minimum pendulum-attractor separation,  $s$ , of  $100 \mu\text{m}$  and a peak-to-peak distance modulation amplitude of  $0.5 \text{ mm}$ . A theoretical Yukawa torque (red dashed curve) with parameters  $\alpha = 1$  and  $\lambda = 100 \mu\text{m}$  would be larger than the Newtonian background (blue solid curve). The table to the right in Figure 5 is the harmonic torque amplitudes for the time series on the left. At  $2\omega$  and  $3\omega$  the Yukawa signals are much greater than the Newtonian torque amplitudes.

### 3. Optical set up and noise performance

For the experiment to effectively measure deviations from the ISL and WEP, an optical system with the ability to measure angles to one nanoradian uncertainty in a day is required to measure the angular twist of the pendulum. The previous autocollimator, Figure 5, consisted of a laser being directed through a beam splitter and then the remaining beam collimated and directed to the pendulum. The returning beam was then focused onto a 10-mm square position-sensitive detector (PSD) which outputs four voltages proportional to the beam's location on the detector. The output voltages are amplified, sent to SR830 lock-in Amplifiers and then sent to the data acquisition board where, by using calibration coefficients, the voltages are used to determine the angular twist of the pendulum.

In order to reduce the noise floor so the desired sensitivity can be achieved, a polarizing beam splitter and a quarter-wave plate were implemented in the autocollimator. With a non-polarizing beam splitter only a quarter of the output beam was being received as signal on the PSD due the beam dump of the beam splitter, where half of the beam was lost each time the beam passed through. With the polarizing beam splitter, all of output beam reaches the PSD as signal. The polarizing beam splitter allows light with an outward linear polarization through to the collimating lens, and the beam from the laser can be oriented in the same polarization so that the entire beam passes through the beam splitter with none of the beam lost to the beam dump. The polarization of the beam is changed to be circular as it passes through the quarter-wave plate. When the beam reflects off the pendulum's surface, the sense of the circular polarization is effectively reversed. As the beam returning from the pendulum's surface passes through the quarter-wave plate the polarization is shifted back to a linear polarization that is perpendicular to the outgoing beam's polarization. The beam with the perpendicular polarization passes through the other side of the beam splitter and is directed onto the PSD. This ensures that the PSD is measuring the angular twist of the pendulum and reduces noise in the optical system since scattered light is reduced and is less likely to be directed toward the PSD. The signal level is also increased since less light is being lost in a beam dump as it goes through the beam splitter. A redesigned PSD circuit with updated components was also installed. A noise spectrum of a benchtop setup of the updated autocollimator, Figure 6, revealed that the noise floor in the optical system had been reduced to the desired sensitivity of the apparatus.

The sensitivity of the experiment is determined by the amount of time,  $t$ , it takes to measure the twist of the pendulum at a given frequency to some angular uncertainty  $\Delta$ ,

$$t = \left( \frac{A}{\Delta} \right)^2, \quad (2)$$

where  $A$  is the noise floor at that frequency in radians/sqrt(Hz). The desired sensitivity of this experiment is to achieve an uncertainty of 1 nanoradian per one day of data. This would require  $A$  to be less than  $3 \times 10^{-7}$  rad/ $\sqrt{\text{Hz}}$  at the frequency of interest. Notice that Equation 2 shows that the uncertainty decreases as the square root of the measurement time as expected.

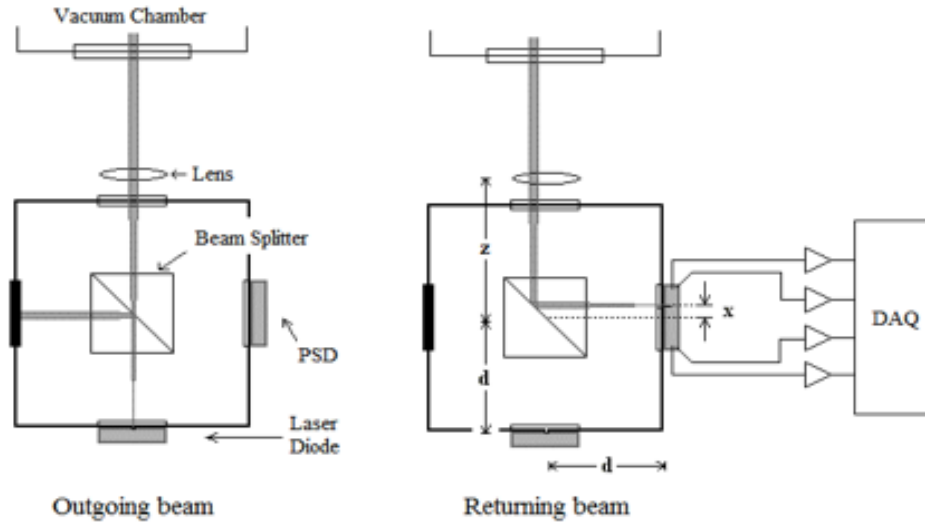


Figure 5. Autocollimator schematic

Figure 5 shows the previous autocollimator setup where an outgoing laser beam is sent through a pinhole and directed through a beam splitter, where half of the light is lost to a beam dump. The beam passing through the beam splitter is then collimated with a lens and directed through a window in the vacuum chamber. The light returning from the pendulum is focused onto the beam splitter where the incoming light is directed to the side with the PSD. The PSD outputs four voltages proportional to the beams location on the PSD. The output voltages are sent into the Labview data acquisition package. The updated autocollimator has a similar configuration with a polarizing beam splitter and a quarter wave plate added between the lens and the beam splitter.

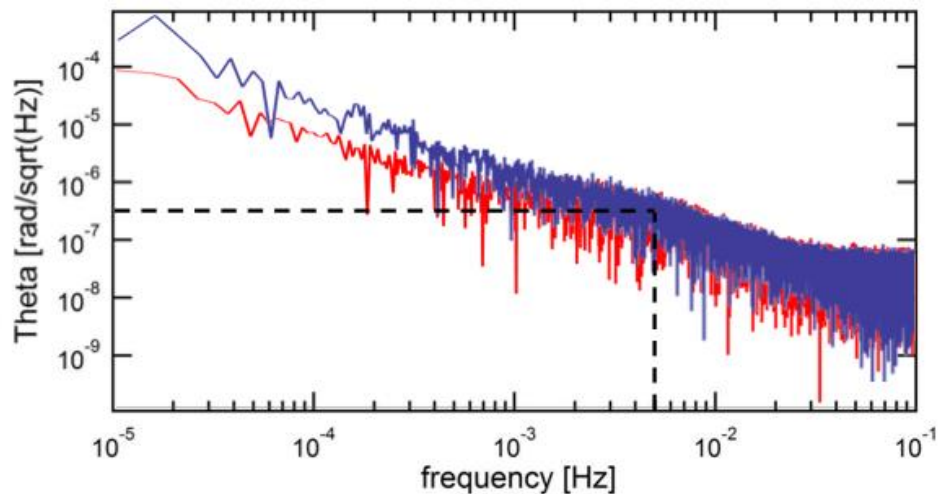


Figure 6. Noise performance of updated autocollimator

In Figure 6, two runs of noise data taken from an updated autocollimator are overlaid atop one another. The data in blue corresponds to data taken from the benchtop setup with the laser on, while the red data corresponds to the noise in the benchtop set up with the laser off. The two agree at high frequencies, and the noise floor,  $A$ , at the frequency of interest, 0.01 Hz, is approximately  $1.2 \times 10^{-7}$  rad/ $\sqrt{\text{Hz}}$ . The black dashed line indicates the noise in the autocollimator at the attractor modulation frequency. For nanoradian per day sensitivity,  $A$  must be less than  $3 \times 10^{-7}$  rad/ $\sqrt{\text{Hz}}$ . This noise floor corresponds to nanoradian uncertainty being achieved in 14400 s, or 4 hours, which exceeds the requirement of achieving nanoradian uncertainty in one day.

## 4. Pendulum and electrostatic control

A set of electrodes placed behind the pendulum, as shown in Figure 7 can produce a torque so that the free oscillation of the pendulum can be controlled and reduced before data acquisition. The applied torque on the pendulum is approximately  $N_{\text{applied}} \approx \frac{1}{2} \frac{\partial}{\partial \theta} (C_1 V_1^2 + C_2 V_2^2)$  where  $C_i$  and  $V_i$  are the capacitances and the applied DC voltage to each electrode and  $\theta$  is the pendulum twist with respect to an equilibrium value. A PID feedback loop uses angular data from the autocollimator to provide the proper voltages to damp oscillation of the pendulum or adjust the equilibrium position of the pendulum twist.

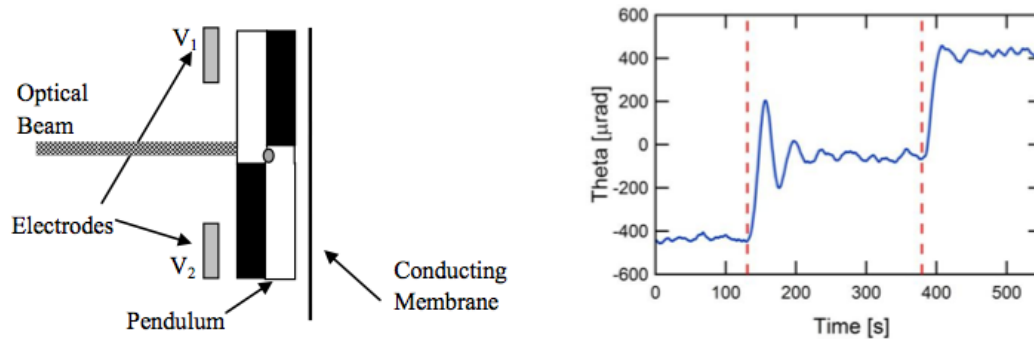


Figure 7. Electrostatic control schematic and damping data

A top view of the pendulum with the electrostatic sensor/actuator is shown in the left of Figure 7. When a DC voltage is applied to either electrode a torque is produced on the pendulum. The right side of Figure 7 shows the angular position of a mock pendulum at atmospheric pressure being controlled by the electrodes and the PID feedback loop. The red dashed lines indicate the times which correspond to approximately  $t = 130\text{s}$  and  $390\text{s}$  where the proportional (set point) and the differential (damping) terms of the PID loop were changed to demonstrate its functionality.

## 5. Flat Mirror Interferometer

Interferometers are very sensitive at measuring small changes in optical path length (OPL) between the two paths of a split coherent beam. When the two beams are recombined an interference pattern occurs that varies corresponding to the difference in OPL between the split beams. A classic and adapted Michelson Interferometer are shown in Figure 8. Changes in the OPL between the two legs of the interferometer can be measured to within a half wavelength of the source since the difference in the OPL between a light fringe and a dark fringe corresponds to a half wavelength change in the interference pattern. When a 632.8 nm He-Ne laser is used as the source one fringe shift corresponds to a change in the OPL of 316.4 nm. For the flat mirror interferometer both legs are directed to either side of a flat mirror that is mounted at its pivot point atop a Newport URS50BPP precision rotation stage that is controlled using a software driver to control to rotation of the stage and the speed of the rotation. From a rough benchtop setup, changes in angle of 17.45 microradians can be resolved in real time.

Two photodiodes separated by half of an interference fringe are used as the detector. The outputs of the photodiodes are sent to an INA 126 differencing amplifier whose output is then connected to the non-inverting input of an LM311 comparator. When the difference between the outputs of the photodiodes is large, the interference pattern is such that the two photodiodes are separated by one half fringe, and the comparator outputs zero volts. When the difference between the photodiodes is small, both photodiodes are on one fringe, and the comparator

outputs five volts. Using LabView, the falling or rising edges of the comparators' output can be counted which corresponds to the number of fringes that have passed by the detector. Counting the number of fringes that passes by the detector yields the change in angle of the flat mirror using Equation 3. For constructive interference,

$$4d = m\lambda, \tag{3}$$

where  $d$  is the optical path difference between the two beams which from geometry is equal to  $d=L \tan(\theta)$  where  $L$  is the distance from the pivot point to the location where the beam hits the mirror. Expanding  $\tan(\theta)$  for small angles, the angle through which the flat mirror pivots can be approximated as

$$\theta = \frac{m\lambda}{4L}. \tag{4}$$

By counting the number of interference fringes that pass by a detector, the change in angle of the flat mirror can be estimated using a series expansion. This interferometer technique is anticipated to be more sensitive at measuring small changes in angle of a flat pendulum than the current autocollimator set up, and is being developed for use with the experimental apparatus in the vacuum.

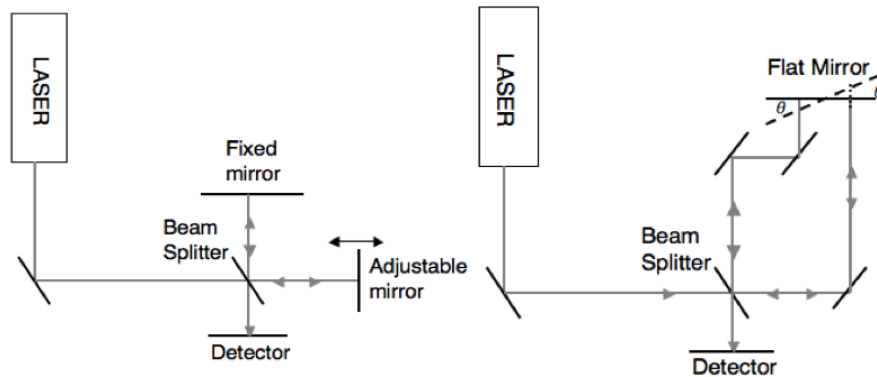


Figure 8. Michelson Interferometer and Adapted Michelson Interferometer

A classic Michelson Interferometer, shown on the left, uses two flat mirrors on either side of a beam splitter with the distance between each mirror and the beam splitter being approximately the same optical path length (OPL). When the split beam recombines after reflecting off of each mirror, an interference pattern occurs due to the difference in the OPL between the two beams. The flat mirror interferometer on the right instead reflects the two beams from either side of a flat mirror that pivots about the center. A polished torsion pendulum would replace the flat mirror for eventual implementation in our experiment.

## 6. Conclusion

We are developing an experiment at Humboldt State that will probe the gravitational ISL and the WEP at untested distance scales. The novel parallel-plate torsion pendulum design will be the most sensitive apparatus to date for measuring gravitational effects at the 20 micron scale. Such a setup requires an incredibly sensitive angle sensor. An optical autocollimator and modified Michelson interferometer are being developed for this task.



In the benchtop setup of the updated autocollimator the electronic noise floor had been reduced so that nanoradian per day sensitivity could be obtained. The complete autocollimator is sensitive enough to measure nanoradian per day pendulum twist, the optical system and is ready to take science quality data. A flat mirror interferometer is being developed to measure small changes in angle of the pendulum and is expected to resolve smaller changes in angle than the current autocollimator system.

## 7. Acknowledgements

We are thankful for financial support from the National Science Foundation (Grant PHY-1065697), Research Corporation (Cottrell College Science Award CC6839), and the Humboldt State University College of Natural Resources and Sciences (CNRS), Office of Research and Graduate Studies, and President's Office. Special thanks to Dr. C.D. Hoyle for his guidance in the Gravitational Research Laboratory.

## 8. References

1. N. Arkani-Hamed, S. Dimopoulos and G.R. Dvali, "New Dimensions at a Millimeter to a Fermi and Superstrings at a TeV," *Phys. Lett. B* 436, 257 (1998).
2. G. Dvali, G. Gabadadze, M. Kolanovic and F. Nitti, "Scales of Gravity," *Phys. Rev. D* 65 (2001) 024031.
3. D.J. Kapner, T.S. Cook, E.G. Adelberger, J.H. Gundlach, B.R. Heckel, C.D. Hoyle, and H.E. Swanson, "Tests of the Gravitational Inverse-Square Law below the Dark-Energy Length Scale," *Physical Review Letters* **98** 021101 (2007).
4. E.G. Adelberger, B.R. Heckel and A.E. Nelson, "Tests of the Gravitational Inverse-Square Law," *Ann. Rev. Nucl. Part. Sci.* **53** (2003) 77. [http://arxiv.org/PS\\_cache/hep-ph/pdf/0307/0307284v1.pdf](http://arxiv.org/PS_cache/hep-ph/pdf/0307/0307284v1.pdf)
5. Andrew A. Geraci, Sylvia J. Smullin, David M. Weld, John Chiaverini, and Aharon Kapitulnik, "Improved constraints on non-Newtonian forces at 10 microns," *Physical Review D* **78**, 022002 (2008).
6. J. K. Hoskins, R. D. Newman, R. Spero, and J. Schultz, "Experimental tests of the gravitational inverse-square law for mass separations from 2 to 105 cm," *Physical Review D* **32**, 3084 (1985).
7. S.-Q. Yang, B.-F. Zhan, Q.-L. Wang, C.-G. Shao, L.-C. Tu, and W.-H. Tan, and J. Luo, "Test of the Gravitational Inverse Square Law at Millimeter Ranges," *Phys. Rev. Lett.* 108, 081101 (2012).  
<http://link.aps.org/doi/10.1103/PhysRevLett.108.081101>